

2021-09-15

Inorganic nitrogen and phosphorus in Western European aerosol and the significance of dry deposition flux into stratified shelf waters

White, C

<http://hdl.handle.net/10026.1/17348>

10.1016/j.atmosenv.2021.118391

Atmospheric Environment

Elsevier BV

All content in PEARL is protected by copyright law. Author manuscripts are made available in accordance with publisher policies. Please cite only the published version using the details provided on the item record or document. In the absence of an open licence (e.g. Creative Commons), permissions for further reuse of content should be sought from the publisher or author.

1 **Inorganic nitrogen and phosphorus in Western European aerosol and the**
2 **significance of dry deposition flux into stratified shelf waters**

3

4 Caroline White^[1], Simon J. Ussher^[1], Mark F. Fitzsimons^[1], Sov Atkinson^[1], E. Malcolm S.
5 Woodward^[2], Mingxi Yang^[2], Thomas G. Bell^[2]

6 [1] Biogeochemistry Research Centre, School of Geography, Earth and Environmental Science,
7 University of Plymouth, Drake Circus, Plymouth, PL4 8AA, UK

8 [2] Plymouth Marine Laboratory, Prospect Place, Plymouth, PL1 3DH, UK

9

10 **ABSTRACT**

11 Dry deposition of nitrogen (N) and phosphorus (P) from the aerosol phase represents a potential
12 source of nutrients to marine surface waters. To investigate the significance of this deposition
13 pathway, aerosol samples were collected from Penlee Point Atmospheric Observatory in SW England,
14 UK, over a 6-month period (February to July 2015) covering the spring bloom. Samples were analysed
15 for nitrate, ammonium and phosphate and the dry deposition flux of these nutrients calculated to
16 assess its potential impact on primary production in nearby surface seawater. Aerosol-derived N and
17 P deposition fluxes ranged from 2.7 - 620 $\mu\text{mol N m}^{-2} \text{d}^{-1}$ and 0.16 - 1.6 $\mu\text{mol P m}^{-2} \text{d}^{-1}$, respectively.
18 Air mass back trajectory analysis indicated that the highest N fluxes were associated with polluted
19 European air masses, highlighting a significant anthropogenic influence on N-content of aerosols. The
20 N:P ratios of aerosol fluxes and water column concentrations indicated that P deposition was unlikely
21 to be biologically significant in the region. In contrast, aerosol deposition was a significant episodic
22 source of new N to marine phytoplankton after the onset of water column stratification. Carbon
23 fixation estimates indicated that the maximum proportion of new primary production sustained by
24 aerosol-N deposition was 22.4 %, a factor of ten higher than the study average. These data suggest

25 that enhanced N-deposition from polluted continental air masses could sustain pulses of surface
26 ocean biological productivity during periods of dissolved N depletion.

27

28 **1. INTRODUCTION**

29 Reactive nitrogen (N) and phosphorus (P) are vital macronutrients in surface seawater, fuelling
30 primary production by marine phytoplankton and the biological carbon pump (Elser *et al.*, 2007).
31 Anthropogenic activities in the last century have created new sources of reactive N and significantly
32 altered the global nitrogen cycle (Duce *et al.*, 2008; Galloway *et al.*, 2003; Martino *et al.*, 2014).
33 Emission model studies estimate a fourfold increase in inorganic nitrogen emissions since 1850 (Duce
34 *et al.*, 2008; Jickells *et al.*, 2017; Krishnamurthy *et al.*, 2009). The Redfield ratio of N to P uptake (16:1)
35 in phytoplankton means that small changes to the P pool can impact the N:P ratio if the system is close
36 to Redfield (Elser *et al.*, 2007).

37 Atmospheric reactive N is made up of inorganic oxidised forms (nitrate, NO_3^- , and nitrite, NO_2^-), and
38 the inorganic reduced form, ammonia/ammonium ($\text{NH}_3/\text{NH}_4^+$), as well as an organic N fraction (Hertel
39 *et al.*, 2012). Atmospheric reactive N in the aerosol phase can be transported long distances from
40 emission sources, potentially spanning continents and ocean basins. From the perspective of primary
41 production, approximately 70% of the surface ocean is N limited or N co-limited with P (Moore *et al.*,
42 2013). Atmospheric deposition can introduce significant pulses of reactive N to N-limited surface
43 waters (Kim *et al.*, 2014; Okin *et al.*, 2011; Owens *et al.*, 1992).

44 Anthropogenic emissions of oxidised N are primarily derived from N oxides from combustion
45 processes such as road transportation, shipping and industry (Hertel *et al.*, 2012; Okin *et al.*, 2011). A
46 large proportion of gas phase N oxides (NO_x) undergo atmospheric transformation to form nitric acid,
47 which displaces chloride on the surface of sea salt particles (typically coarse mode, $>1 \mu\text{m}$ diameter)
48 in the marine boundary layer (Ottley & Harrison, 1992; Yeatman, Spokes & Jickells, 2001). Emissions

49 of reduced N are predominately from agricultural sources, as well as from biomass burning (Hertel *et*
50 *al.*, 2012; Okin *et al.*, 2011). Gas phase NH₃ is very soluble and readily protonates in the aqueous phase
51 of the aerosol to form the NH₄⁺ ion. Nitric acid also reacts with NH₃ to form fine mode (<1 µm diameter)
52 ammonium nitrate aerosol (Yeatman, Spokes & Jickells, 2001).

53 Jickells *et al.* (2017) estimated global inorganic nitrogen emissions as ca. 100 Tg N yr⁻¹. Reactive N
54 emission estimates for Europe were reported by Leip *et al.* (2011): NO_x emissions totalled 3.5 Tg N yr⁻¹
55 and were dominated by road transport (1.3 Tg N yr⁻¹) and combustion from industry (1.0 Tg N yr⁻¹).
56 Reduced N (NH₃/NH₄⁺) emissions totalled 3.2 Tg N yr⁻¹ and were dominated by agriculture at 3.0 Tg N
57 yr⁻¹ (Leip *et al.*, 2011). Hence, the emission ratio of oxidised and reduced N species both in Europe and
58 globally is estimated to be approximately 1:1 even though the sources are not the same.

59 Phosphorus is mainly emitted to the atmosphere as aerosol (Myriokefalitakis *et al.*, 2016). The
60 principal sources include mineral dust (48 %), anthropogenic (14 %) and biogenic emissions (34 %;
61 from plants, animals and bacteria). Total P in the atmosphere predominately comprises insoluble
62 mineral dusts, orthophosphates, soluble and insoluble organic P (Myriokefalitakis *et al.*, 2016).
63 Orthophosphate (PO₄³⁻) is the most common and bioavailable form of soluble P in the ocean (Björkman
64 & Karl, 2003; Mahowald *et al.*, 2008). Mahowald *et al.*, (2008) estimated that 0.74 Tg of PO₄³⁻ is
65 released to the atmosphere each year across the globe. These global estimates, which are derived
66 from a wealth of past measurements, e.g. Baker *et al.*, (2006; 2007; 2010; 2017), suggest that
67 anthropogenic activity has not significantly altered aerosol PO₄³⁻ concentrations. Based on the global
68 estimates for N and P emissions (Jickells *et al.*, 2017; Mahowald *et al.*, 2008) the global atmospheric
69 N:P ratio is greater than 400, hence it can further be concluded that globally the aerosol phase is N
70 rich compared to P.

71 Atmospheric deposition can provide an important additional source of soluble N to marine surface
72 waters under certain conditions. Previous studies observed several significant N deposition events
73 from air masses originating from Europe and estimated that N deposition could support up to 30 % of

74 new daily primary production in the NE Atlantic Ocean (Spokes *et al.*, 2000; Spokes and Jickells, 2005).
75 In seasonally stratified waters during the spring/summer months, water column stratification can trap
76 nutrients within a limited depth range in the sunlit euphotic zone, which facilitates phytoplankton
77 growth but can also isolate them from remineralised nutrient sources at depth. Sustained biological
78 activity draws down available nutrients to the point where external inputs of N (e.g. from atmospheric
79 deposition) have the potential to be highly significant (Chester & Jickells, 2012; Spokes & Jickells, 2005;
80 Spokes *et al.*, 2000; Owens *et al.*, 1992). However, it must be noted that stratification within the water
81 column is a dynamic feature which varies in depth and can even be broken down by strong physical
82 processes (e.g. winds, currents). A complete breakdown in stratification allows nutrients trapped in
83 the deep shelf water to be mixed throughout the water column, thus resupplying the surface with
84 nutrients, including bioavailable N and P (Schmidt *et al.*, 2020; Maier *et al.*, 2012; Lentz *et al.*, 2003).

85 Carbon flux and carbon fixation measurements in coastal and shelf regions, during seasons with active
86 primary production, have shown that wet and dry deposition of N can contribute 0.4 – 3.7 % of new
87 primary production (Park *et al.*, 2019; Kocak, 2015; Singh *et al.*, 2012). Even in regions of significant
88 wind driven upwelling such as the Californian coastline, atmospheric N-deposition is estimated to
89 account for up to 8 % of new productivity (Mackey *et al.*, 2010). The largest impact of atmospheric N
90 deposition has been found in regions of high population density and air pollution. In the SE China
91 coastline, 5.6 – 19.4 % of new primary production is supported by N-deposition from nearby
92 anthropogenic sources during winter and summer seasons (Wang *et al.*, 2019). These studies
93 demonstrate that increased inputs of reactive nitrogen to coastal regions from anthropogenic sources
94 will have significant impact on coastal marine primary production in the future, as predicted by several
95 global modelling studies (Duce *et al.*, 2008; Baker *et al.*, 2017).

96 The aim of this study was to integrate atmospheric aerosol and marine nutrient observations at a well-
97 studied coastal time-series site in order to estimate the impact of atmospheric reactive soluble N and
98 P deposition on seasonally stratified shelf waters. The study site is situated on the south-west coast

99 of England, UK, and uses atmospheric time-series data from Penlee Point Atmospheric Observatory
100 (PPAO) and seawater time-series data from the Western Channel Observatory (WCO). The data were
101 collected between February and July 2015, spanning the period of water column stratification and the
102 phytoplankton spring bloom.

103 **2. METHODS**

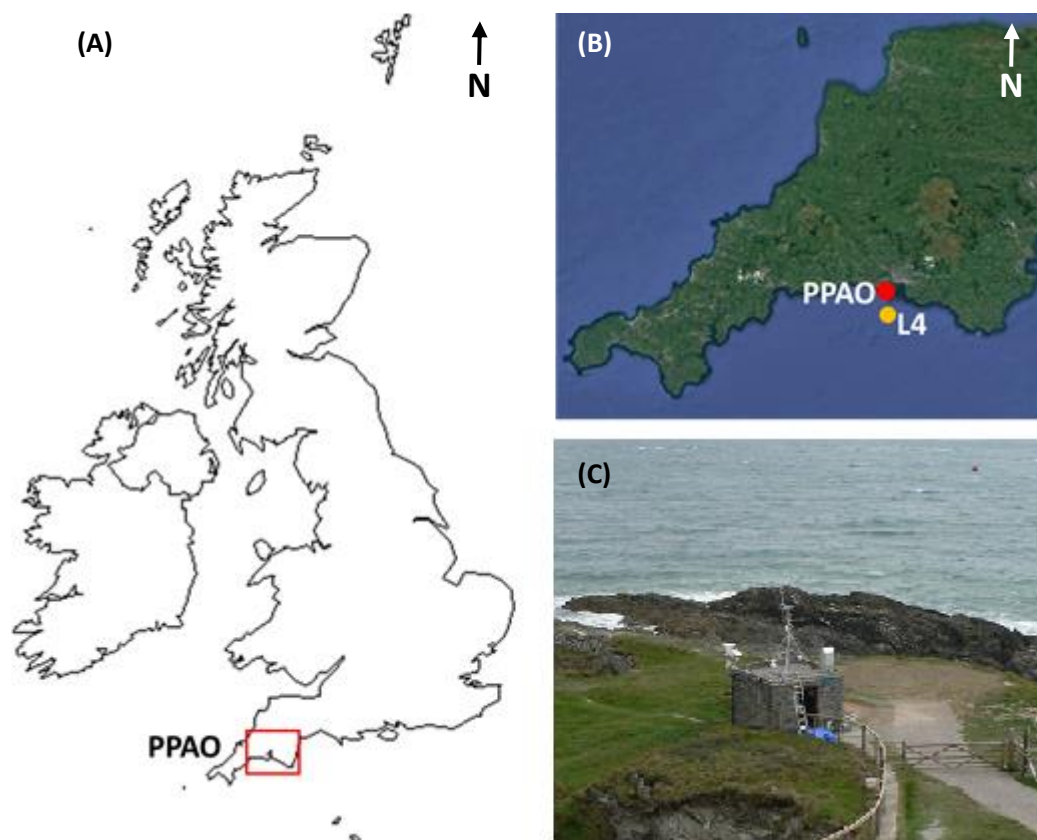
104 Atmospheric data were collected from the PPAO, situated on the Rame Head Peninsula on the western
105 edge of Plymouth Sound, Cornwall, UK (50°19.080 N, 4°11.350 W). The coastal site is exposed to a
106 number of distinct wind sectors/air masses, including the North Atlantic Ocean from the southwest,
107 and mainland Europe/ship emission within the English Channel from the east/southeast (Figure 1).
108 The PPAO was established in 2014 by Plymouth Marine Laboratory (PML) in collaboration with the
109 University of Plymouth and detail on the site characteristics is presented elsewhere (Yang *et al.*, 2019;
110 Yang *et al.*, 2016a; Yang *et al.*, 2016b). Gas phase carbon dioxide, methane, sulfur dioxide, ozone and
111 meteorological variables (wind speed, wind direction, relative humidity, atmospheric pressure and
112 rain rate) are continuously monitored. Aerosol samples were collected weekly and analysed at the
113 University of Plymouth (UoP) for inorganic nutrients.

114 Seawater samples and data were collected from L4, a long-term coastal monitoring buoy located 6 km
115 south of PPAO (50°15.00' N, 4°13.02' W). L4 is a key sampling station for the Western Channel
116 Observatory (WCO, <http://www.westernchannelobservatory.org.uk>). Continuous measurements at
117 the L4 buoy include PAR, sea surface temperature, salinity and chlorophyll. Routine weekly water
118 column samples are collected from L4 for nutrient concentrations (NO_2^- , NO_3^- , NH_4^+ , PO_4^{3-}),
119 (Woodward & Harris, 2019), and are analysed in a shore-based laboratory by a SEAL Analytical
120 segmented flow autoanalyzer using colorimetric analysis techniques (Woodward & Rees, 2001).
121 Concurrent temperature and salinity profiles are collected weekly by CTD from the RV Plymouth
122 Quest.

123

124

125



126

127 **Figure 1:** (A) Location of study area. (B) Location of Penlee Point Atmospheric Observatory (PPAO) and
128 of the Western Channel Observatory marine time series L4 station/buoy. (C) Site in Spring 2015 (photo
129 taken facing south). Aerosol samples were collected from a Hi-Vol sampler positioned on the SW corner
130 of the roof of the building.

131 **Aerosol Sampling and Analysis**

132 Particulate aerosol samples were collected onto acid-cleaned and combusted 8 x 10" (203 x 254 mm)
133 Whatman Quartz Microfiber Filters (QMA) using a Tisch Environmental (model TE-5170) high-volume
134 aerosol sampler (approximately 1 m³ min⁻¹ flow rate), which was calibrated in accordance with the
135 product handbook using a manometer once a month. Samples (n = 22) were collected weekly from 9th
136 February to 14th July 2015. Filters were pre-loaded into an aluminium filter cassette for sampling and

137 protected by an aluminium cover until sampling began. There was a sampling gap from 5th-26th March
138 due to a sampler malfunction. During the sampling days, air was filtered for either 24 hours (9th
139 February-9th April) or 12 hours (9th April-14th July). Filter samples were collected and sealed in zip-lock
140 bags, then transported in an insulated container for storage (-20 °C freezer) and analysis at the UoP
141 laboratory. Aerosol filters samples were prepared for analysis by subsampling into quarters and
142 submerging one subsample in 125 mL of high purity water (HPW; $\geq 18.2 \text{ M}\Omega \text{ cm}$) overnight to leach
143 the soluble N and P into solution (Cornell & Jickells, 1999). Leaching efficiency was assessed by
144 performing a second extraction on sub-samples. All analytes of secondary extractions were below the
145 limit of detection, confirming high efficiency of the initial single extraction.

146 Aerosol NO_2^- , NO_3^- and PO_4^{3-} were determined by spectrophotometric analysis based on Hansen and
147 Koroleff, (2007) and Gardolinski *et al.*, (2001), using a continuous flow, air-segmented nutrient auto
148 analyser (Skalar SAN^{plus} series 1074). Instrumental precision was determined from the relative
149 standard deviation (RSD) of triplicate measurements. Mean RSD for $\text{NO}_3^- + \text{NO}_2^-$ was 2.84 % (n = 22),
150 and for PO_4^- was 1.34 % (n = 22), which is consistent with inter-comparison studies involving the same
151 instrument (Birchill *et al.*, 2019). Concentrations of NO_2^- for aerosols are typically below detection
152 limits (approx. 0.1 nmol m^{-3} : Baker *et al.*, 2010; Lesworth, Baker & Jickells, 2010), so this small fraction
153 (< 4% maximum: 0.2% median) was combined with NO_3^- and reported as aerosol NO_3^- . Ammonium
154 (NH_4^+) was analysed by fluorimetry, using a Hitachi F-4500 fluorometer (see Holmes *et al.*, 1999). Air
155 concentrations were calculated by dividing the detected values by the total volume of air that had
156 passed through the filter.

157 **Dry Deposition Fluxes**

158 Dry deposition fluxes were calculated to investigate the importance of aerosol as a source of nutrients
159 to coastal waters (Spokes & Jickells, 2005). Here, fluxes are calculated as daily (24 h) inputs, hence the
160 airmass concentrations collected over a 12 h period have been interpolated as a constant 24 h

161 concentration. The deposition flux (Equation 1) is the product of the aerosol concentration (C) and the
162 deposition velocity (V_d):

$$163 \quad \text{Flux} = C V_d \quad (1)$$

164 The deposition velocity is influenced by physical processes such as gravitational settling, impaction
165 and diffusion, which are constrained by particle size, wind speed and sea surface conditions (Duce *et al.*,
166 1991). The deposition velocity is not well quantified (Baker *et al.*, 2010; Duce *et al.*, 1991) and
167 there is a large uncertainty on current estimates. We used a particle size-dependent V_d value: 2.0 cm
168 s^{-1} for coarse mode particles (diameter > 1 μm) and 0.1 cm s^{-1} for fine mode particles (diameter < 1
169 μm) (Duce *et al.*, 1991; Slinn & Slinn, 1980). These V_d values were chosen to enable comparison with
170 other studies (e.g. Spokes & Jickells, 2005; Yeatman *et al.*, 2001).

171 Samples collected from PPAO were not size-segregated, so it was necessary to estimate the relative
172 distribution of NO_3^- , NH_4^+ and PO_4^{3-} within the fine and coarse mode aerosol. PO_4^{3-} sources
173 predominantly generate larger sized (> 1 μm) aerosols, with the exception of combustion sources
174 which can either be greater or less than 1 μm (Myriokefalitakis *et al.*, 2016; Mahowald *et al.*, 2008).
175 Combustion sources represent approximately 14 % of global aerosol PO_4^{3-} (Mahowald *et al.*, 2008), so
176 we assume that all aerosol PO_4^{3-} was in the coarse mode and apply a deposition velocity of 2.0 cm s^{-1} ,
177 appropriate to >1 μm particle sizes to calculate the deposition flux (Duce *et al.*, 1991). Defining size
178 distributions for NO_3^- and NH_4^+ is more challenging as previous studies have shown that coarse and
179 fine mode ratios of NO_3^- and NH_4^+ are highly dependent on source region (Bencs *et al.*, 2009; Spokes
180 & Jickells, 2005; Yeatman *et al.*, 2001). PPAO is situated between two well- established atmospheric
181 observatories, Mace Head, Galway (Ireland) and Weybourne, Norfolk (UK). Mace Head and
182 Weybourne are exposed to the same air mass sectors described at PPAO and size segregated NO_3^- and
183 NH_4^+ measurements have been made for these sectors (Spokes & Jickells, 2005; Yeatman *et al.*, 2001).
184 We used the Mace Head and Weybourne data (Table 1) to estimate the size distribution of NO_3^- and

185 NH_4^+ in the air masses encountered at PPAO for this study. The uncertainty related to this estimation
186 has been taken into account in any discussion of fluxes.

187 **Table 1:** Percentage medians (\pm range) of coarse mode ($> 1\mu\text{m}$) NO_3^- and NH_4^+ found in aerosols from
188 source region extrapolated from Spokes & Jickells (2005) and Yeatman *et al* (2001).

Source Region	$> 1\mu\text{m NH}_4^+$	$> 1\mu\text{m NO}_3^-$
N Atlantic Clean	18.5 % ($\pm 17.5\%$)	70 % ($\pm 21\%$)
N Atlantic Mixed	20.5 % (± 5.5)	65 % ($\pm 12\%$)
Channel Mixed	36.5 % ($\pm 0.5\%$)	69 % ($\pm 1\%$)
Continental	43.5 % ($\pm 1.5\%$)	48.5 ($\pm 8.5\%$)

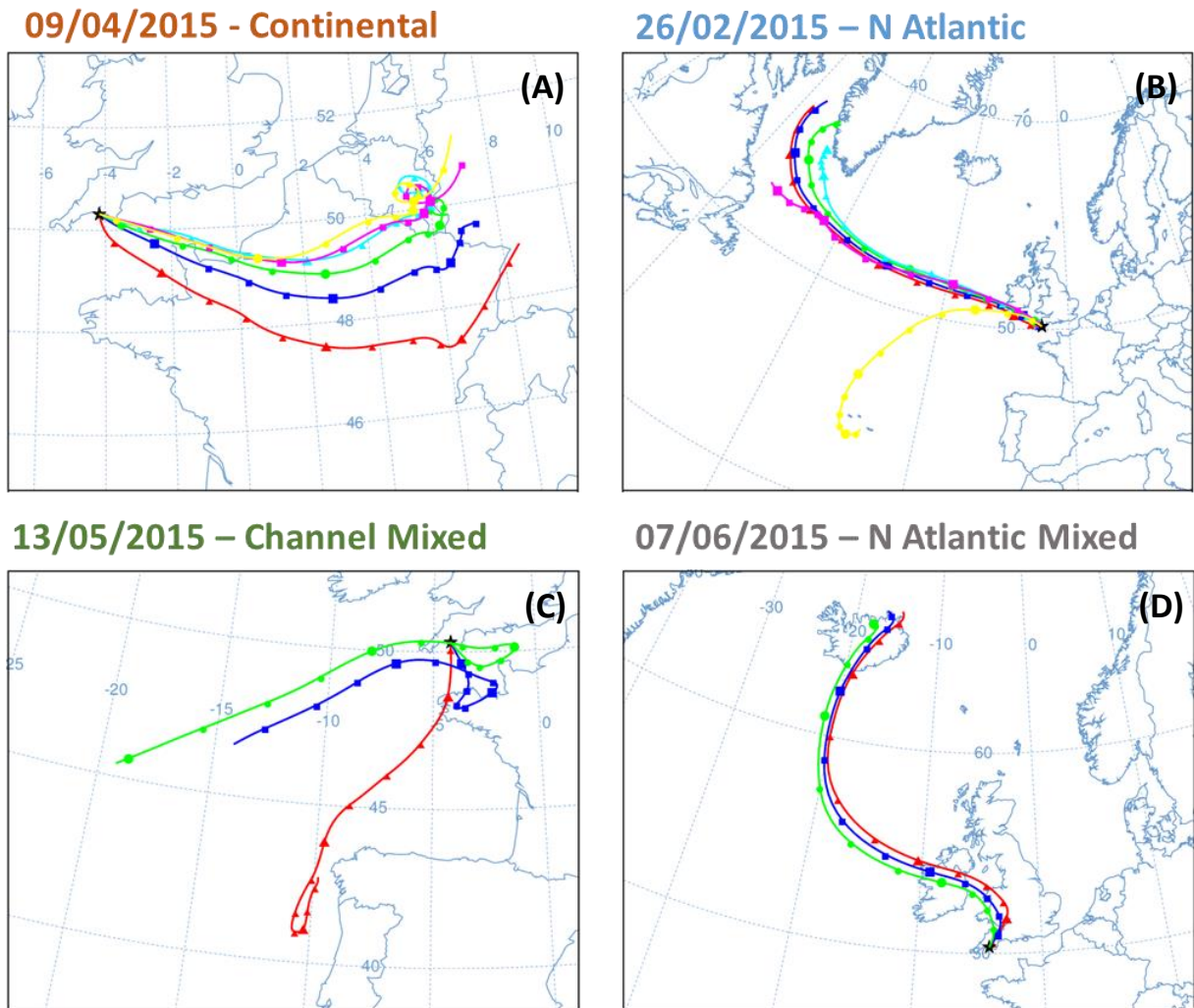
189

190 Source Region Analysis

191 Wind sectors have been defined previously for PPAO using the local wind direction (Yang *et al.*, 2016a).
192 In this study, we combined the local wind direction with air mass back trajectory analysis to categorise
193 the source region of each aerosol sample. Air mass back trajectories were calculated using the
194 National Oceanic and Atmospheric Administration (NOAA) HYbrid Single-Particle Lagrangian
195 Integrated Trajectory (HYSPLIT) model (<http://ready.arl.noaa.gov/HYSPLIT.php>). A back trajectory was
196 calculated every 6 hours while the aerosol sampler was running, resulting in 3 trajectories for 12 hour
197 samples and 6 trajectories for 24 hour samples. Trajectories were initiated at 20 m above ground level
198 and run backwards for 72 hours.

199 Each sample was classified into one of four air mass source regions using the local wind speed and
200 direction (Yang *et al.*, 2016a) and its HYSPLIT back trajectory. The four wind sectors are the
201 Continental, North Atlantic, Channel Mixed and N Atlantic Mixed (see examples in Figure 2). The
202 predominant wind direction at PPAO is from the West/South-West, and the North Atlantic Ocean is
203 the dominant influence on this air (North Atlantic). Air from the West and North-West often originates

204 over the North Atlantic, but has spent time over Ireland and rural parts of the UK prior to reaching the
 205 PPAO (N Atlantic Mixed). Winds from the East/South-East have been influenced by ship emissions in
 206 the English Channel and anthropogenic/terrestrial emissions from continental Europe (Continental).
 207 During low wind speed events, the air tends to stagnate in the local area, picking up a mixture of ship
 208 and marine emissions (Channel Mixed).



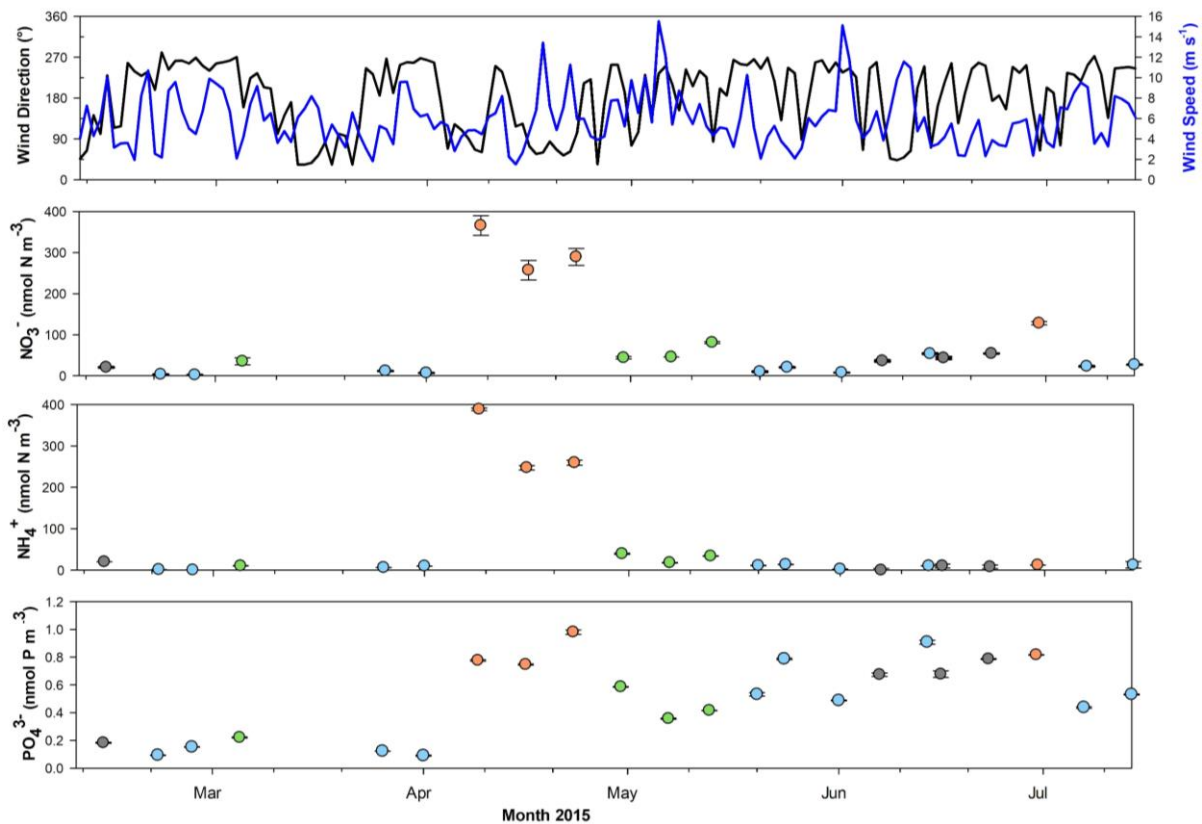
209

210 **Figure 2:** Example back trajectories for the four sectors defined for this study. Multiple trajectories
 211 were run per sample (different colour lines). Symbols represent 6 hour intervals along the trajectory.

212 **3. RESULTS**

213 **3.1 Penlee Point Atmospheric Observatory Aerosols**

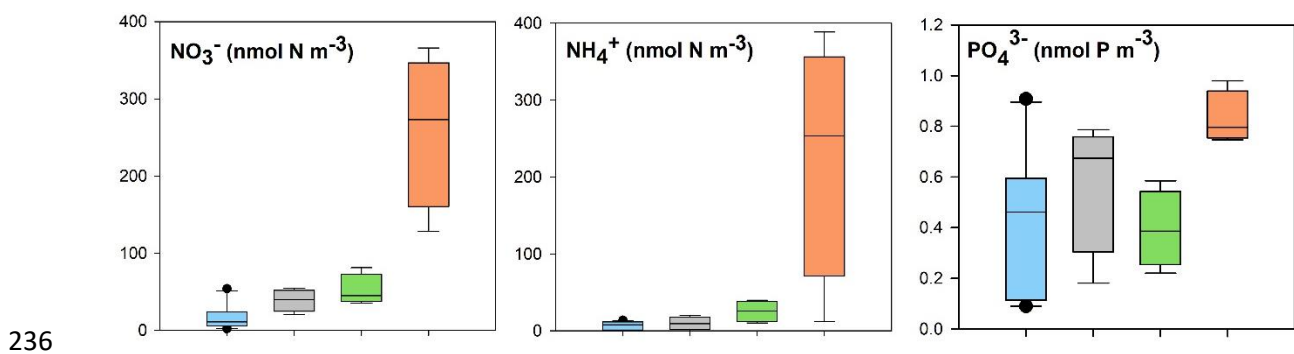
214 Air mass NO_3^- concentrations varied from 2–366 nmol N m^{-3} , with the minimum and maximum
 215 occurred on 26th February and 9th April, respectively (Figure 3; Figure 4). The highest aerosol NO_3^-
 216 concentrations were observed in air masses from continental Europe/UK Mainland, and these were
 217 associated with an easterly local wind direction (Figure 4). NO_3^- concentrations associated with this
 218 source region also had the greatest concentration range (128 – 366 nmol N m^{-3}). In contrast, low
 219 aerosol NO_3^- concentrations were observed in North Atlantic clean aerosols (2–27 nmol N m^{-3}) except
 220 on the 16th June (43 nmol N m^{-3}). Low wind speeds prevailed during sample collection on the 16th June,
 221 and the back trajectory suggests that the air mass circulated over the Celtic Sea and English Channel.
 222 Hence it is likely this aerosol sample had entrained emissions from the intense shipping activity in
 223 these waters.



224
 225 **Figure 3:** Timeseries of aerosol inorganic N (NO_3^- and NH_4^+ , nmol N m^{-3}) and PO_4^{3-} (nmol P m^{-3})
 226 concentrations, wind speed (m s^{-1}) and local wind direction (degrees) between 9th February and 14th
 227 July 2015. Points are coloured by source region classification: North Atlantic Clean (blue), Continental

228 (orange), Channel Mixed (green) and North Atlantic Mixed (grey). Major tick marks represent the 1st
229 of the month and minor tick marks represent 10th and 20th days.

230 Aerosol NH₄⁺ concentrations ranged from 0.21 – 389 nmol N m⁻³ and tended to co-vary with NO₃⁻
231 concentrations (Figure 3). Continental aerosols had the highest NH₄⁺ concentrations. One exception
232 was on 30th June 2015, when NH₄⁺ concentrations were 12.2 nmol N m⁻³, which is more comparable
233 with background North Atlantic samples than with other Continental samples. The NO₃⁻ concentration
234 in the same sample was approximately 50% of the other three Continental samples. Back trajectory
235 analysis shows that the air had circulated in the English Channel for 72 hours prior to sampling.

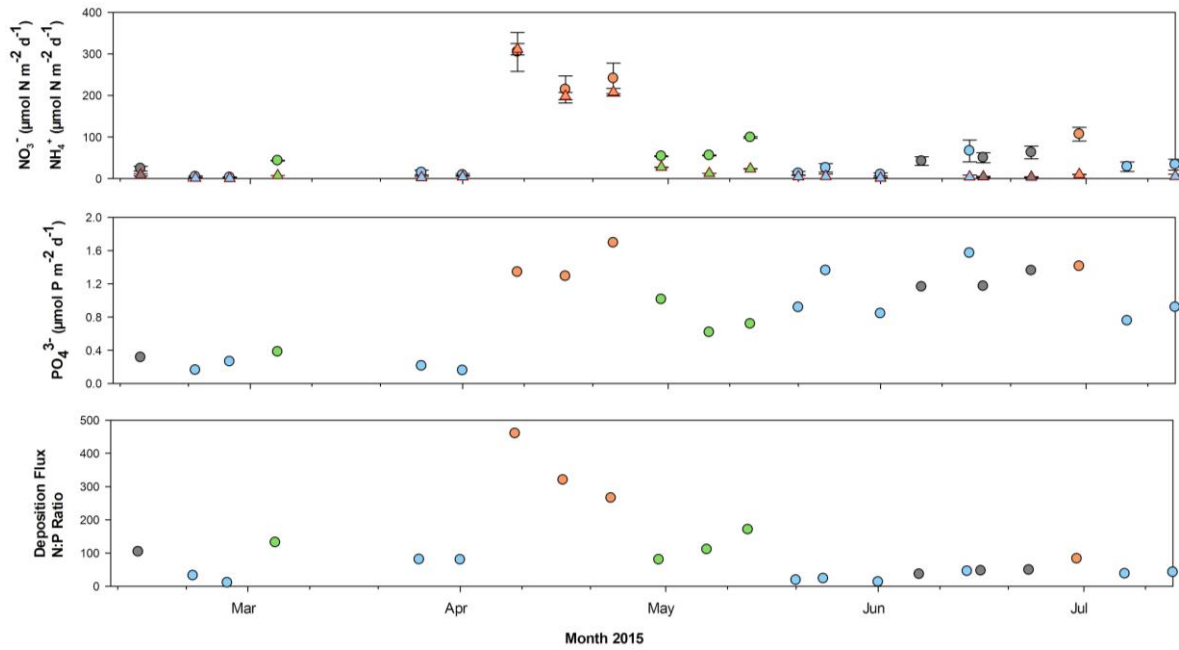


236
237 **Figure 4:** Box and whisker plots of aerosol NO₃⁻, NH₄⁺ and PO₄³⁻ concentrations, coloured by source
238 region classification: North Atlantic clean (blue, 10 samples), Continental (orange, 4 samples), Channel
239 Mixed (green, 4 samples) and North Atlantic Mixed (grey, 4 samples).

240

241 Aerosol phosphate (PO₄³⁻) concentration ranged from 0.1 – 1.0 nmol P m⁻³. The lowest concentrations
242 were recorded on 21st February and 1st April 2015, and the highest occurred on 23rd April (Figure 4).
243 PO₄³⁻ was considerably less abundant than aerosol nitrogen, and there was no clear link between the
244 PO₄³⁻ concentrations and air mass classification or variations in inorganic nitrogen concentration.
245 Mineral and soil dusts are the major source of soluble P for aerosol. These are typically larger particles
246 with short atmospheric residence times. Thus, atmospheric P concentrations are likely to be
247 dependent on localised continental sources rather than long range transport (Myriokefalitakis *et al.*,

248 2016). Average (mean and median) aerosol PO_4^{3-} concentrations in air masses from the European
 249 Continent/UK were elevated (Figure 4) compared to other source regions, especially North Atlantic
 250 Clean and Channel Mixed. Concentrations from the North Atlantic Mixed region were also slightly
 251 elevated, suggesting terrestrial influence as the trajectories passed over South West England and
 252 South East Ireland.



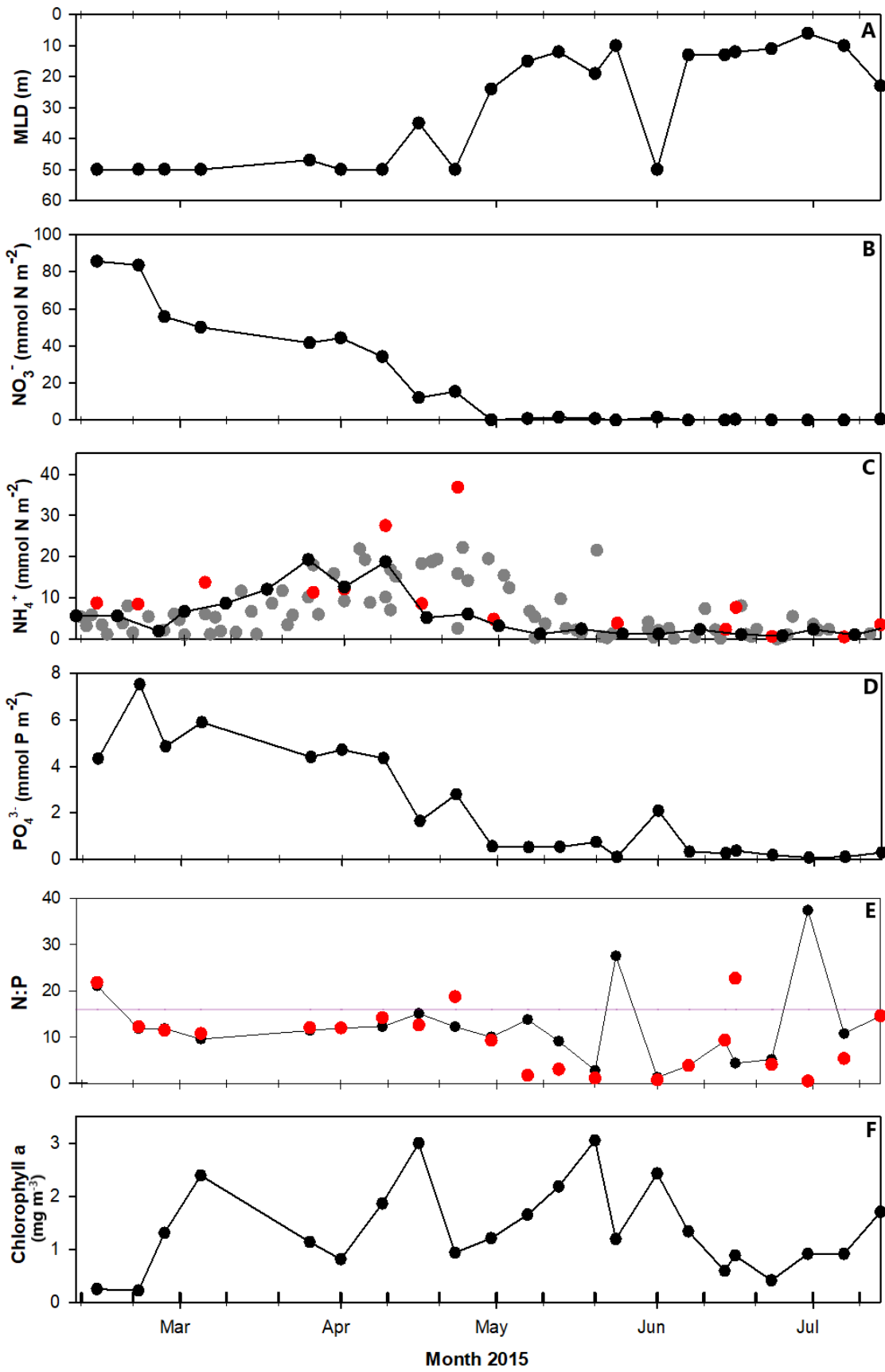
253
 254 **Figure 5:** Dry deposition fluxes for NO_3^- , NH_4^+ and PO_4^{3-} ($\mu\text{mol N/P m}^{-2} \text{d}^{-1}$) and the N:P ratio of the
 255 aerosol depositing on the sea surface. Circles and triangles in the top panel represent nitrogen fluxes
 256 resulting from NO_3^- and NH_4^+ respectively. Points are coloured by back trajectory source regions: North
 257 Atlantic Clean (blue), Continental (orange), Channel Mixed (green) and North Atlantic Mixed (grey).
 258 Error bars on NO_3^- and NH_4^+ show the maximum/minimum deposition using the coarse/fine size
 259 distribution ranges in Table 1. Major tick marks represent the 1st of the month and minor tick marks
 260 represent 10th and 20th days.

261 Average NO_3^- and NH_4^+ deposition flux were $68 (\pm 12)$ and $38 (\pm 3) \mu\text{mol N m}^{-2} \text{d}^{-1}$ respectively.
 262 Deposition fluxes ranged from $3 (\pm 1)$ to $300 (\pm 47) \mu\text{mol N m}^{-2} \text{d}^{-1}$ for NO_3^- and $0.01 (\pm 0.03)$ to 310
 263 $(\pm 14) \mu\text{mol N m}^{-2} \text{d}^{-1}$ for NH_4^+ . The N:P ratio of the aerosol deposition flux (Figure 5) demonstrates that

264 N deposition far exceeds P deposition, with most samples exceeding 50:1 N:P ratio. Only 1 sample
265 period had an N:P ratio in the deposited aerosol that fell below the Redfield ratio in seawater (16:1) .

266 **3.2 Trends in marine mixed layer nutrients in the Western English Channel**

267 Vertical nutrient profiles from the Western Channel Observatory L4 marine time series site were
268 integrated down to the base of the spring/summer mixed layer. A pycnocline formed during spring
269 from May onwards, and the average depth was 16 m (\pm 11 m). A mixed layer depth was defined for
270 each profile using a \pm 0.03 kg m³ density difference starting at 3 m. Nutrient profiles were integrated
271 down to the seabed (54 m) prior to stratification (Figure 6).



273 **Figure 6:** WCO L4 timeseries for spring bloom period in 2015. (A) Mixed layer depth used for nutrient
274 integration, derived as $\pm 0.03 \text{ kg m}^{-3}$ from density profiles calculated from CTD temperature & salinity
275 profiles (1 atm) starting at 3m. (B, C, D) Integrated mixed layer nutrient concentrations (NO_3^- , NH_4^+ ,
276 PO_4^{3-}), (E) mixed layer N:P ratio and (F) Chlorophyll a (mg m^{-3}) concentration at the surface. Grey dots
277 on NH_4^+ plot are data from 2016-2019, red dots are for data from 2015 and the black dots/black line
278 shows the median trend of all these NH_4^+ data. Major tick marks represent the 1st of the month and
279 minor tick marks represent 10th and 20th days.

280 The water column was fully mixed at the WCO between 9th February and 7th April 2015. Stable
281 stratifications occurred April 30th at which point the mean mixed layer depth (MLD) was 17 m (± 11
282 m). Stratification was broken down once during the bloom season on June 1st. Mixed layer nutrients
283 reduced significantly during the spring/summer months, reflecting the typical seasonal pattern of
284 phytoplankton growth and nutrient utilisation in these waters (Statham *et al.*, 2012). Mixed layer NO_3^-
285 ranged from 0.01–85.6 mmol N m^{-2} , with minima and maxima measured on 7th June and 9th February,
286 respectively (Figure 6). NO_3^- decreased to a low level ($< 5 \text{ nmol N m}^{-2}$) on 27th April 2015 and remained
287 low for the remainder of the campaign.

288 Surface layer NH_4^+ ranged from 0.5 - 36.8 mmol N m^{-2} and did not follow exactly the same trend as
289 NO_3^- (Figure 6). Water column measurements of NH_4^+ during the 2015 campaign were inconsistently
290 reported after the water column stratifies (Figure 6). To mitigate this uncertainty, a median seasonal
291 trend for NH_4^+ concentrations was derived from all available WCO data from 2015 – 2019 (Figure 6).
292 There are three distinct stages to the seasonal NH_4^+ concentration changes: (i) concentrations are low
293 until mid-March because, unlike NO_3^- and PO_4^- , winter stocks are low; (ii) NH_4^+ concentrations increase
294 almost three fold at the onset of the spring bloom and before stratification, with some inter-annual
295 variation, indicating a biological turnover source of NH_4^+ , e.g. NH_4^+ production due to grazing by
296 zooplankton communities (Alcaraz, Saiz & Estrada, 1994); (iii) concentration decline to winter levels

297 after stratification, with occasional spikes, possibly due to secondary blooms or another point source
298 (e.g. river Tamar inputs).

299 Surface layer PO_4^{3-} ranged from 0.06 to 7.5 mmol P m^{-2} , with the minimum and maximum measured
300 on 30th June and February 9th 2015, respectively. The decline in PO_4^{3-} levels reflects the seasonal
301 nutrient depletion also observed in the dissolved inorganic nitrogen (DIN, = $\text{NO}_3^- + \text{NH}_4^+$) levels (Figure
302 6). The majority of observed N:P ratios at the WCO L4 site were below the expected Redfield ratio (i.e.
303 < 16:1), meaning that PO_4^{3-} was predominately in excess (Figure 6). Excess PO_4^{3-} indicates that, with
304 sufficient light, addition of N to the system could stimulate greater biological productivity. Only when
305 there are elevated NH_4^+ concentrations in the water column does the N:P ratio rise above 16, which
306 could have led to P limitation within the phytoplankton community. P-limitation (or stress) at the WCO
307 has been measured previously following an influx of N-rich fresh water from the River Tamar, through
308 an increase in alkaline phosphatase activity (Rees *et al.*, 2009).

309 **4. DISCUSSION**

310 The N dry deposition fluxes presented in this study are of a similar magnitude to measurements
311 elsewhere in western Europe during the past 20 years. Nitrogen ($\text{NO}_3^- + \text{NH}_4^+$) dry deposition flux at
312 PPAO ranged from 2.7 (± 1.1) to 620 (± 60) $\mu\text{mol N m}^{-2} \text{d}^{-1}$, which is similar to the range reported from
313 a coastal atmospheric station in De Haan, Belgium (7.86 – 405 $\mu\text{mol N m}^{-2} \text{d}^{-1}$; (Bencs *et al.*, 2009)).
314 The large N dry deposition event from 9th-23rd April 2015 was much higher than the fluxes observed
315 during the 1996/1997 sampling campaign at Mace Head, Ireland (9.3–203 $\mu\text{mol N m}^{-2} \text{d}^{-1}$ (Spokes *et*
316 *al.*, 2000)). PPAO is closer than Mace Head to continental Europe, which may explain this difference.
317 Yeatman *et al.*, (2001) collected aerosols from continental air masses at Weybourne (on the coast of
318 the North Sea, South East UK). The authors observed dry deposition fluxes between 166 and 1545
319 $\mu\text{mol N m}^{-2} \text{d}^{-1}$. Weybourne and the southern North Sea are very close (< 400 km) to the industrial
320 heartland of mainland Europe and thus more exposed than the PPAO/WCO to large N deposition
321 events. Other factors will have influenced the observations outlined above, including: (i) time that air

322 masses spend over industrial and agricultural regions; (ii) changing emission source strengths; (iii)
323 different relative proportions of wet versus dry deposition; and (iv) different atmospheric chemical
324 and physical processing.

325 Minimum NO_3^- and NH_4^+ concentrations were observed in North Atlantic Clean air masses. Maximum
326 NO_3^- and NH_4^+ concentrations were observed when air came from Continental Europe (Figure 4).
327 Interestingly, though NO_3^- and NH_4^+ emission sources are different, we observed that aerosol
328 concentrations in Continental Europe samples co-varied and had a relatively constant 1:1 ratio (See
329 Supplementary material). The aerosol concentration ratio may be determined by a similar average
330 ratio in the emissions from the European continent. Indeed, estimated N emissions from continental
331 European countries reported that annual average oxidised and reduced N emissions were also
332 approximately 1:1 (Leip *et al.*, 2011). Several samples were noted to have back trajectories that
333 traverse regions of high shipping density, which will contribute additional NO_3^- but not NH_4^+ (Hertel *et*
334 *al.*, 2012). In contrast with inorganic N fluxes, PO_4^{3-} dry deposition flux varied far less (one order of
335 magnitude), most likely due to a more consistent local source in the form of mineral dusts and soils,
336 rather than an integrated concentration over greater transport distances. Marine sources are not as
337 significant: Baker *et al.*, (2010) reported only 0.98– 4.89 $\text{nmol P m}^{-2} \text{d}^{-1}$ dry phosphate fluxes in the
338 middle of the North Atlantic Ocean (~3 orders of magnitude lower than this study). The significant
339 difference is likely due to the proximity of PPAO to crustal source material and the association of PO_4^{3-}
340 with coarse mode aerosols that have a much shorter atmospheric residence time (Duce *et al.*, 1991).
341 PO_4 concentrations are low when polluted air masses came from Continental Europe, possibly because
342 the low residence time of larger dust aerosols reduces the significance of non-arid source regions far
343 from the sampling site. Furthermore, PO_4^{3-} air mass concentrations are typically low and it is
344 challenging to accurately distinguish between the relative contribution of natural and anthropogenic
345 sources to the low levels of aerosol PO_4^{3-} measured in this study.

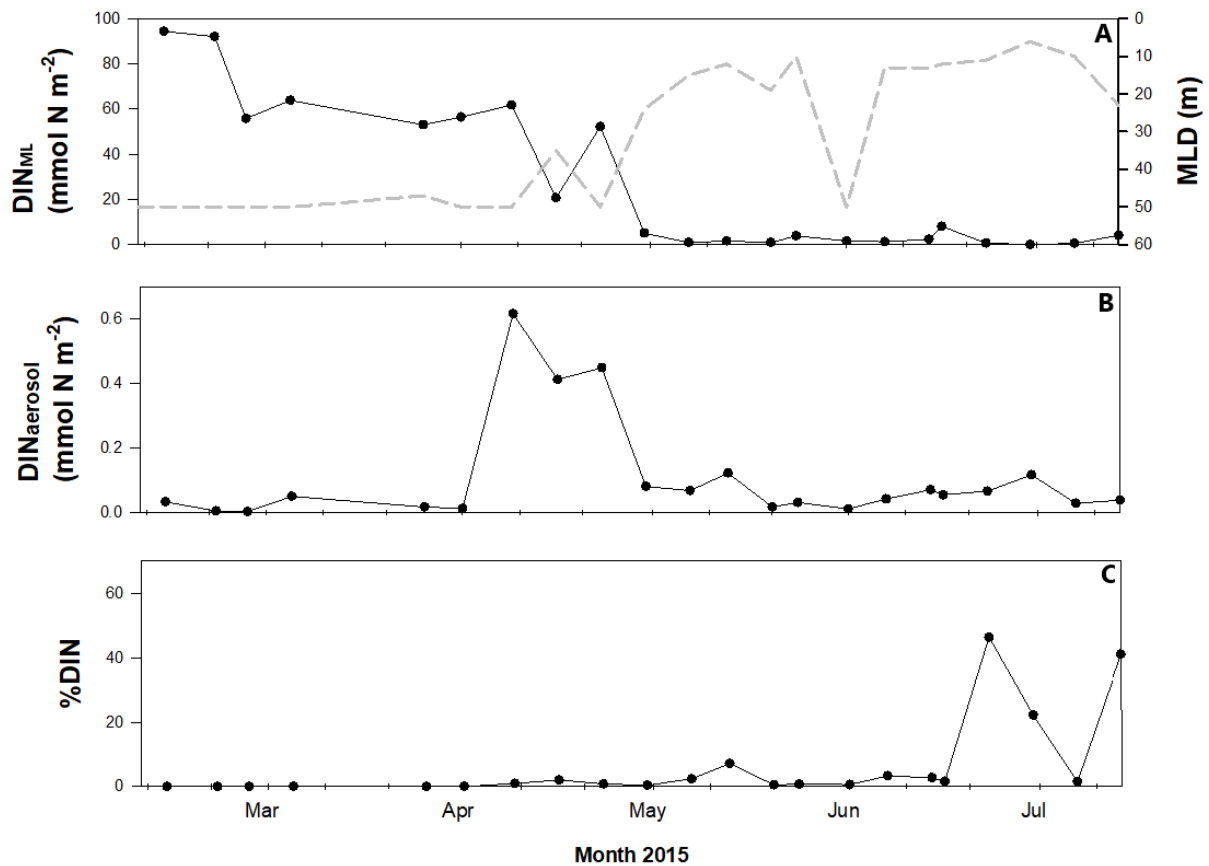
346 **Impact of atmospheric aerosol deposition on surface mixed layer nutrients**

347 Oceanic data from the WCO L4 marine time-series station and atmospheric data from the PPAO were
348 used to assess the potential impact of aerosol nutrients on the local seawater (Figure. 7). As an
349 indicator, a simple 1-D approach to compare the atmospheric aerosol N flux in one day ($DIN_{Aerosol}$) to
350 the standing stock of DIN integrated to the base of the MLD/seabed (DIN_{ML}) as a percentage (%DIN):

$$351 \quad \%DIN = 100 \times DIN_{Aerosol} / DIN_{ML} \quad (2)$$

352 This approach was initially applied to dry aerosol PO_4^{3-} deposition but the contributions were
353 consistently below 0.1 %. Therefore, all further discussion of the response of the WCO L4 site to
354 aerosol nutrient deposition and the potential biogeochemical consequences will focus on N
355 deposition.

356 The water column was mixed down to the seabed prior to 13th April 2015, and DIN_{ML} levels were high
357 ($>10 \text{ mmol N m}^{-2}$) such that aerosol deposition had very little impact on seawater DIN ($\%DIN < 1 \%$,
358 Figure 7). The onset of stratification around 1st May 2015 led to strong biological uptake and reduced
359 DIN_{ML} levels to below 10 mmol N m^{-2} . The $DIN_{Aerosol}$ in early May was classified as Channel Mixed and
360 this aerosol contributed up to 8% of DIN_{ML} . DIN_{ML} was almost completely depleted ($< 10 \text{ mmol N m}^{-2}$)
361 during June 2015 and after this time, deposition events resulted in %DIN exceeding 20% (Figure 7).



362

363 **Figure 7:** Timeseries of: (A) Mixed layer dissolved inorganic nitrogen (DIN_{ML}), grey line is MLD used for
 364 integration; (B) total aerosol dry nitrogen deposition flux ($DIN_{Aerosol}$); and (C) contribution of dry
 365 deposition to water column inorganic N (%DIN, see text for how calculated). Major tick marks represent
 366 the 1st of the month and minor tick marks represent 10th and 20th days.

367 The deposition event on June 30th 2015 had the biggest potential impact and contributed almost 23 %
 368 of DIN_{ML} at the WCO L4 station (Figure 7). Remarkably, %DIN was not significant during the very high
 369 $DIN_{Aerosol}$ deposition events (Continental air masses) in April 2015 because the water was not yet
 370 stratified and nutrient stocks were not depleted (Figure 7). Thus, sporadic atmospheric aerosol N
 371 deposition can be significant source of nitrogen to shelf waters when DIN_{ML} is depleted during periods
 372 of stratification and intense biological activity. Atmospheric circulation patterns are not tied to the
 373 onset of stratification, however previous studies from PPAO have shown that winter dominance of
 374 SW (marine) air masses is reduced in spring/summer allowing for more Continental air masses to occur

375 (Yang *et al.*, 2019; Yang *et al.*, 2016a; Yang *et al.*, 2016b). Had the high $DIN_{Aerosol}$ inputs occurred in May
376 rather than in April, the % DIN would have been 14–37 %. Therefore, continental air masses have the
377 potential to significantly influence the late spring and summer phytoplankton bloom at the WCO.

378 Another relative comparison can be made between aerosol deposition and vertical water column
379 fluxes across the seasonal thermocline to the mixed layer. Summertime diffusive fluxes of NO_3^- across
380 the stratified thermocline in the nearby Celtic Sea are $1.8 - 2 \text{ mmol } NO_3^- \text{ m}^{-2} \text{ d}^{-1}$ (Birchill *et al.*, 2017;
381 Sharples *et al.*, 2009). Hence the maximum dry deposition event observed at PPAO was equivalent to
382 around a third of the typical daily diffusive flux across the thermocline.

383 **Carbon fixation due to aerosol deposition into coastal waters**

384 The assimilation of one mole of reactive nitrogen leads to 6.625 moles of carbon assimilation
385 according to Redfield stoichiometry (106C : 16N : 1P; (Geider and La Roche, 2002; Redfield, 1958)).
386 To calculate carbon fixation related to aerosol N deposition, we assume that all $DIN_{Aerosol}$ was
387 bioavailable and that the other requirements for biological growth (other macro- and micro-nutrients,
388 light, temperature) were met. The $DIN_{Aerosol}$ contribution of $0.02 - 0.62 \text{ mmol N m}^{-2} \text{ d}^{-1}$ during this
389 study was potentially able to support $0.01 - 4.36 \text{ mmol C m}^{-2} \text{ d}^{-1}$ of carbon uptake (Figure 8A).

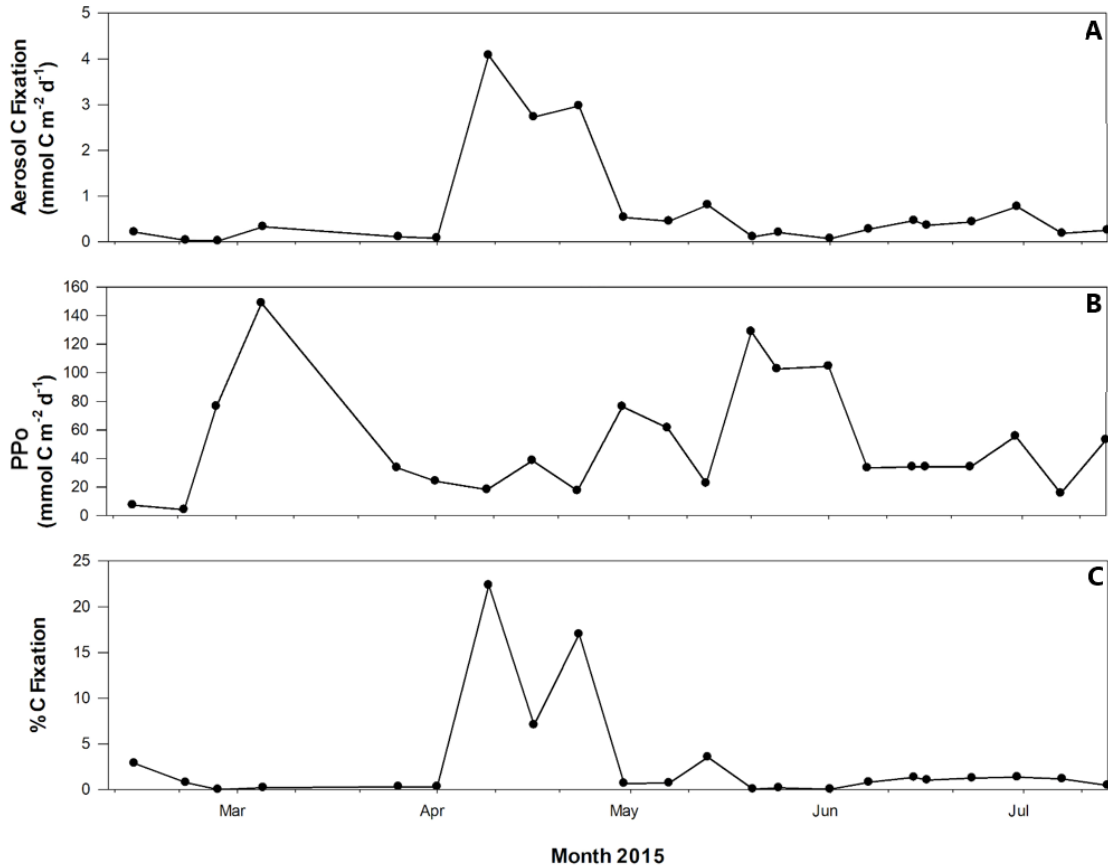
390 Previous studies have compared the potential carbon fixation due to $DIN_{Aerosol}$ to the seasonal average
391 carbon fixation in the North Atlantic Ocean (Bencs *et al.*, 2009, Spokes and Jickells, 2005). These
392 studies observed that dry N deposition derived from continental European air masses could account
393 for up to 15 % of the daily C fixation in the N E Atlantic Ocean (Bencs *et al.*, 2009, Spokes and Jickells,
394 2005). Barnes *et al.*, (2015) report seasonal C-fixation rates and estimates for the WCO L4 station
395 between 2003 and 2010. The average C- fixation rate during the season phytoplankton bloom at the
396 WCO is $43.3 \text{ mmol C m}^{-2} \text{ d}^{-1}$ (Barnes *et al.*, 2015). We estimate C-fixation at the WCO L4 site (PP_o) using
397 in situ chlorophyll observations (Barnes *et al.*, 2014) (Figure 8B):

$$398 \quad \alpha_{ph} = 0.0134 \times \text{Chl a} \times 0.0075 \quad (3)$$

399

$$PP_o = 0.0109 \times (\alpha_{ph} \times E_{par}) - 0.00018 \quad (4)$$

400 Where α_{ph} is absorption coefficient of phytoplankton, and E_{par} is photosynthetically active radiation.



401

402 **Figure 8:** Timeseries of: (A) Carbon fixation due to $DIN_{Aerosol}$ input ($Cfix_{Aerosol}$), assuming uptake follows
 403 the phytoplankton Redfield ratio; (B) Carbon fixation (PP_o) at the Western Channel Observatory L4
 404 station estimated from in situ observations (see Eqn. 3); and (C) Proportion of PP_o at L4 that could be
 405 supported by atmospheric N deposition, assuming all $DIN_{Aerosol}$ is bioavailable ($\%Cfix = 100 \times Cfix_{Aerosol} /$
 406 PP_o). Major tick marks represent the 1st of the month and minor tick marks represent 10th and 20th
 407 days.

408 We compared C-fixation (PP_o) at the WCO with the C-fixation that could potentially be supported by
 409 aerosol N deposition ($Cfix_{Aerosol}$) using $\%Cfix = 100 \times Cfix_{Aerosol} / PP_o$ (Figure 8C). The typical $\%Cfix$ was
 410 $\sim 1\%$. The $\%Cfix$ resulting from continental aerosol deposition during April was 15.5% on average, with

411 dry N deposition on April 9th potentially able to support a substantial amount of the mixed layer carbon
412 fixation ($\%C_{fix} = 22.4\%$).

413 Overall, these recent data highlight the continuation of high sporadic atmospheric nitrogen fluxes
414 originating from air circulation over highly populated land masses and the impact they can have on
415 surface ocean biogeochemistry. Spokes and Jickells, (2005) also reported significant wet and dry
416 nitrogen deposition ($0.8 \text{ mmol m}^{-2} \text{ d}^{-1}$) at Mace Head, Ireland, when air had been transported over the
417 European continent. Bencs *et al.*, (2009) reported a similar magnitude deposition event at De Haan,
418 Belgium. Both studies calculate that episodic deposition events containing polluted European aerosol
419 could support ~15 % of total surface water carbon fixation (Bencs *et al.*, 2009, Spokes and Jickells,
420 2005). The magnitude of N deposition is a function of both location (proximity to aerosol N sources)
421 and prevailing wind direction. Neither of the events observed in Ireland or Belgium deposited as much
422 N as the PPAO event on April 9th 2015.

423 **Impact of N Deposition on Atlantic Shelf Waters**

424 In the previous sections the impact of dry N deposition to the coastal shelf waters near PPAO have
425 been evaluated and revealed two separate conclusions. While the carbon fixation estimates the
426 deposition events in April (corresponding to the highest atmospheric aerosol N concentrations) to
427 have the greatest impact, this was not the case when those deposition events were compared to the
428 standing nutrient stocks. From that investigation we conclude that N deposition has the most impact
429 once the nutrient stocks are depleted during the summer (June onwards) bloom season. Considered
430 together these calculations show that the impact of dry N deposition can have significance, but only
431 when certain conditions are met. However this also highlights the complexity of the cycling of
432 nutrients from the atmospheric into marine surface waters, and there are certainly other factors to
433 investigate in future work at this study site. For instance, the calculation we used to estimate the
434 contribution of $DIN_{Aerosol}$ to DIN_{ML} (Eqn. 2) assumes that DIN_{ML} is at steady state and does not consider
435 the potential importance of other N input and output terms due to uptake and removal processes.

436 Riverine input, atmospheric wet deposition, and diffusive fluxes of nitrogen across the thermocline
437 may all influence DIN cycling in WCO waters.

438 Rainfall will play an important role for coastal and shelf N deposition during the seasons. For example,
439 heavy rainfall over the River Tamar catchment has been shown to increase the freshwater flux of DIN
440 into the English Channel, influencing the WCO L4 site. DIN concentrations at L4 after freshwater influx
441 events in 2007 increased by $1.78 \pm 0.20 \mu\text{mol L}^{-1}$, coinciding with lowered salinity and increased P
442 stress (Rees *et al.*, 2009).

443 Preliminary NO_3^- data in rainwater from PPAO show concentrations in the range of 5.6 - 49 $\mu\text{mol L}^{-1}$.
444 Rainfall efficiently scavenges atmospheric aerosol such that wet N deposition is typically greater than
445 dry N deposition and is likely to add a further significant seasonal flux to the shelf nitrogen budget.
446 The studies in Ireland and Belgium measured twofold higher flux of wet deposition than dry deposition
447 (Bencs *et al.*, 2009, Spokes and Jickells, 2005). Thus, the total atmospheric N deposition in the WCO
448 during our study would have been of higher magnitude if rainfall were considered, particularly as there
449 were 9 major rain events at the PPAO during April 2015. Furthermore, organic N aerosol was not
450 measured in this study, but reports from elsewhere suggest that it may represent 15 – 65 % of the
451 total atmospheric N budget (e.g., Jickells *et al.*, 2013), so the effect of organic N deposition on marine
452 biogeochemistry is likely to be even larger. Thus, the combined impact of dry plus wet N deposition
453 and additional fluxes of organic nitrogen on shelf water biogeochemistry, clearly warrant further
454 investigation.

455 **5. Conclusions**

456 This study investigated atmospheric aerosol N and P, their sources and the potential impact on surface
457 water biogeochemistry at the WCO between February and July 2015. The highest concentrations of N
458 in aerosol were linked to pollution sources in continental Europe. These aerosol samples contained
459 significantly more N than samples from other source regions, and likely contribute substantial pulses
460 of new N into surface waters at the WCO. These shelf waters were N-limited throughout the spring

461 bloom season, and severe N-depletion generally occurred after the onset of water column
462 stratification in spring. Aerosol N deposition always exceeded aerosol P deposition (N:P ratio > 250 in
463 polluted continental European air mass samples) and N:P was also greater than the typical seawater
464 ratio (i.e., Redfield >16:1). Calculations demonstrate that aerosol-derived had the greatest impact on
465 biological productivity in shelf waters once the water column became stratified and during sustained
466 winds from mainland Europe, more than 20 % of water column carbon fixation can be supported by
467 aerosol N deposition.

468

469 **Acknowledgements:**

470 This research was supported by a European Commission Marie Curie Career Integration Grant for
471 S.J.U. (PCIG-GA-2012-333143 DISCOSAT), UK Natural Environment Research Council (NERC)
472 (NE/K001779/1, NE/P021336/1) and a QR-funded University of Plymouth Scholarship. The
473 contribution of T.G.B. and the WCO/PPAO are supported by funding from NERC specifically National
474 Capability (Climate Linked Atlantic Sector Science, CLASS) for the WCO, ACSIS (The North Atlantic
475 Climate System Integrated Study; NE/N018044/1) and ACRUISE (Atmospheric Composition and
476 Radiative forcing changes due to UN International Ship Emissions regulations, NE/S005390/1) for
477 PPAO. We are grateful to Trinity House (<http://www.trinityhouse.co.uk/>) for access and use of the
478 Penlee building and to Mount Edgcumbe Estate (<http://www.mountedgcumbe.gov.uk/>) for providing
479 access to the PPAO site. This is contribution no. 9 from the PPAO.

480

481 **References**

482 Alcaraz, M., Saiz, E. & Estrada, M. (1994) 'Excretion of ammonia by zooplankton and its potential
483 contribution to nitrogen requirements for primary production in the Catalan Sea (NW
484 Mediterranean)'. *Marine Biology*, 119 (1), pp. 69-76.

485

486 Baker, A. R. and Jickells, T. D. (2017) 'Atmospheric deposition of soluble trace elements along the
487 Atlantic Meridional Transect (AMT)', *Progress in Oceanography*, 158, pp. 41-51.

488

489 Baker, A. R., Lesworth, T., Adams, C., Jickells, T. D. & Ganzeveld, L. (2010) 'Estimation of atmospheric
490 nutrient inputs to the Atlantic Ocean from 50°N to 50°S based on large-scale field sampling: Fixed
491 nitrogen and dry deposition of phosphorus'. *Global Biogeochemical Cycles*, 24 (3),

492

493 Baker, A. R., Weston, K., Kelly, S. D., Voss, M., Streu, P. & Cape, J. N. (2007) 'Dry and wet deposition of
494 nutrients from the tropical Atlantic atmosphere: Links to primary productivity and nitrogen fixation'.
495 *Deep Sea Research Part I: Oceanographic Research Papers*, 54 (10), pp. 1704-1720.

496

497 Baker, A. R., Jickells, T. D., Biswas, K. F., Weston, K. and French, M. (2006) 'Nutrients in atmospheric
498 aerosol particles along the Atlantic Meridional Transect', *Deep Sea Research Part II: Topical Studies in
499 Oceanography*, 53(14–16), pp. 1706-1719.

500

501 Barnes, M. K., Tilstone, G. H., Suggett, D. J., Widdicombe, C. E., Bruun, J., Martinez-Vicente, V. & Smyth,
502 T. J. (2015) 'Temporal variability in total, micro- and nano-phytoplankton primary production at a
503 coastal site in the Western English Channel'. *Progress in Oceanography*, 137 pp. 470-483.

504

505 Barnes, M. K., Tilstone, G. H., Smyth, T. J., Suggett, D. J., Astoreca, R., Lancelot, C. and Kromkamp, J. C.
506 (2014) 'Absorption-based algorithm of primary production for total and size-fractionated
507 phytoplankton in coastal waters', *Marine Ecology Progress Series*, 504, pp. 73-89.

508

509 Bencs, L., Krata, A., Horemans, B., Buczyńska, A. J., Dirtu, A. C., Godoi, A. F. L., Godoi, R. H. M.,
510 Potgieter-Vermaak, S. & Van Grieken, R. (2009) 'Atmospheric nitrogen fluxes at the Belgian coast:
511 2004–2006'. *Atmospheric Environment*, 43 (24), pp. 3786-3798.

512

513 Birchill, A. J., Clinton-Bailey, G., Hanz, R., Mawji, E., Cariou, T., White, C., Ussher, S. J., Worsfold, P. J.,
514 J, Achterberg, E., P and Mowlem, M. (2019) 'Realistic measurement uncertainties for marine
515 macronutrient measurements conducted using gas segmented flow and Lab-on-Chip
516 techniques', *Talanta*, 200, pp. 228-235.

517

518 Birchill, A. J., Milne, A., Woodward, E. M. S., Harris, C., Annett, A., Rusiecka, D., Achterberg, E. P.,
519 Gledhill, M., Ussher, S. J., Worsfold, P. J., Geibert, W. and Lohan, M. C. (2017) 'Seasonal iron depletion
520 in temperate shelf seas', *Geophysical Research Letters*, 44(17), pp. 8987-8996.

521

522 Björkman, K. M. & Karl, D. M. (2003) 'Bioavailability of dissolved organic phosphorus in the euphotic
523 zone at Station ALOHA, North Pacific Subtropical Gyre'. *Limnology and Oceanography*, 48 (3), pp.
524 1049-1057.

525

526 Chester, R. & Jickells, T. (2012) 'The Transport of Material to the Oceans: The Atmospheric Pathway',
527 *Marine Geochemistry*. John Wiley & Sons, Ltd, pp. 52-82.

528

529 Cornell, S. E. & Jickells, T. D. (1999) 'Water-soluble organic nitrogen in atmospheric aerosol: a
530 comparison of UV and persulfate oxidation methods'. *Atmospheric Environment*, 33 (5), pp. 833-840.

531

532 Duce, R. A., LaRoche, J., Altieri, K., Arrigo, K. R., Baker, A. R., Capone, D. G., Cornell, S., Dentener, F.,
533 Galloway, J., Ganeshram, R. S., Geider, R. J., Jickells, T., Kuypers, M. M., Langlois, R., Liss, P. S., Liu, S.
534 M., Middelburg, J. J., Moore, C. M., Nickovic, S., Oschlies, A., Pedersen, T., Prospero, J., Schlitzer, R.,

535 Seitzinger, S., Sorensen, L. L., Uematsu, M., Ulloa, O., Voss, M., Ward, B. & Zamora, L. (2008) 'Impacts
536 of Atmospheric Anthropogenic Nitrogen on the Open Ocean'. *Science*, 320 (5878), pp. 893-897.
537

538 Duce, R. A., Liss, P. S., Merrill, J. T., Atlas, E. L., Buat-Menard, P., Hicks, B. B., Miller, J. M., Prospero, J.
539 M., Arimoto, R., Church, T. M., Ellis, W., Galloway, J. N., Hansen, L., Jickells, T. D., Knap, A. H., Reinhardt,
540 K. H., Schneider, B., Soudine, A., Tokos, J. J., Tsunogai, S., Wollast, R. & Zhou, M. (1991) 'The
541 atmospheric input of trace species to the world ocean'. *Global Biogeochemical Cycles*, 5 (3), pp. 193-
542 259.
543

544 Elser, J. J., Bracken, M. E. S., Cleland, E. E., Gruner, D. S., Harpole, W. S., Hillebrand, H., Ngai, J. T.,
545 Seabloom, E. W., Shurin, J. B. & Smith, J. E. (2007) 'Global analysis of nitrogen and phosphorus
546 limitation of primary producers in freshwater, marine and terrestrial ecosystems'. *Ecology Letters*, 10
547 (12), pp. 1135-1142.

548 Galloway, J. N., Aber, J. D., Erisman, J. W., Seitzinger, S. P., Howarth, R. W., Cowling, E. B. & Cosby, B.
549 J. (2003) 'The Nitrogen Cascade'. *Bioscience*, 53 (4), pp. 341-356.
550

551 Gardolinski, P. C. F. C., Hanrahan, G., Achterberg, E. P., Gledhill, M., Tappin, A. D., House, W. A. &
552 Worsfold, P. J. (2001) 'Comparison of sample storage protocols for the determination of nutrients in
553 natural waters'. *Water Research*, 35 (15), pp. 3670-3678.
554

555 Geider, R. & La Roche, J. (2002) 'Redfield revisited: variability of C:N:P in marine microalgae and its
556 biochemical basis'. *European Journal of Phycology*, 37 (1), pp. 1-17.
557

558 Hansen, H. P. & Koroleff, F. (2007) 'Determination of nutrients', *Methods of Seawater Analysis*. Wiley-
559 VCH Verlag GmbH, pp. 159-228.
560

561 Hertel, O., Skjøth, C. A., Reis, S., Bleeker, A., Harrison, R. M., Cape, J. N., Fowler, D., Skiba, U., Simpson,
562 D., Jickells, T., Kulmala, M., Gyldenkerne, S., Sørensen, L. L., Erismann, J. W. & Sutton, M. A. (2012)
563 'Governing processes for reactive nitrogen compounds in the European atmosphere'. *Biogeosciences*,
564 9 (12), pp. 4921-4954.

565

566 Holmes, R. M., Aminot, A., K rouel, R., Hooker, B. A. & Peterson, B. J. (1999) 'A simple and precise
567 method for measuring ammonium in marine and freshwater ecosystems'. *Canadian Journal of*
568 *Fisheries and Aquatic Sciences*, 56 (10), pp. 1801-1808.

569

570 Jickells, T. D., Buitenhuis, E., Altieri, K., Baker, A. R., Capone, D., Duce, R. A., Dentener, F., Fennel, K.,
571 Kanakidou, M., LaRoche, J., Lee, K., Liss, P., Middelburg, J. J., Moore, J. K., Okin, G., Oschlies, A., Sarin,
572 M., Seitzinger, S., Sharples, J., Singh, A., Suntharalingam, P., Uematsu, M. & Zamora, L. M. (2017) 'A
573 reevaluation of the magnitude and impacts of anthropogenic atmospheric nitrogen inputs on the
574 ocean'. *Global Biogeochemical Cycles*, 31 (2), pp. 289-305.

575

576 Kim, T.-W., Lee, K., Duce, R. & Liss, P. (2014) 'Impact of atmospheric nitrogen deposition on
577 phytoplankton productivity in the South China Sea'. *Geophysical Research Letters*, 41 (9), pp. 3156-
578 3162.

579

580 Kocak, M. (2015) 'Solubility of Atmospheric Nutrients over the Eastern Mediterranean: Comparison
581 between Pure-Water and Sea-Water, Implications Regarding Marine Production', *Turkish Journal of*
582 *Fisheries and Aquatic Sciences*, 15, pp. 59-71.

583

584 Krishnamurthy, A., Moore, J. K., Mahowald, N., Luo, C., Doney, S. C., Lindsay, K. & Zender, C. S. (2009)
585 'Impacts of increasing anthropogenic soluble iron and nitrogen deposition on ocean biogeochemistry'.
586 *Global Biogeochemical Cycles*, 23 (3), pp. n/a-n/a.

587

588 Leip, A., Achermann, B., Billen, G., Bleeker, A., Bouwman, A. F., De Vries, W., Dragosits, U., Döring, U.,
589 Fernall, D., Geupel, M., Herolstab, J., Johnes, P., Le Gall, A. C., Monni, S., Nevečeřal, R., Orlandini, L.,
590 Prud'homme, M., Reuter, H. I., Simpson, D., Seufert, G., Spranger, T., Sutton, M. A., Van Aardenne, J.,
591 Voß, M. & Winiwarter, W. (2011) 'Integrating nitrogen fluxes at the European scale', in Sutton, M.A.,
592 Howard, C.M., Erisman, J.W., Billen, G., Bleeker, A., Grennfelt, P., Van Grinsven, H. and Bruna, G. (eds.)
593 *The European Nitrogen Assessment: Sources, Effects and Policy Perspectives*. Cambridge: Cambridge
594 University Press.

595

596 Lentz, S., Shearman, K., Anderson, S., Plueddemann, A. and Edson, J., (2003) 'Evolution of
597 stratification over the New England shelf during the Coastal Mixing and Optics study, August 1996–
598 June 1997.' *Journal of Geophysical Research*, 108 (C1), pp. 1-14

599

600 Lesworth, T., Baker, A. R. & Jickells, T. (2010) 'Aerosol organic nitrogen over the remote Atlantic
601 Ocean'. *Atmospheric Environment*, 44 (15), pp. 1887-1893.

602

603 Mackey, K. R. M., van Dijken, G. L., Mazloom, S., Erhardt, A. M., Ryan, J., Arrigo, K. R. and Paytan, A.
604 (2010) 'Influence of atmospheric nutrients on primary productivity in a coastal upwelling
605 region', *Global Biogeochemical Cycles*, 24(4).

606

607 Mahowald, N., Jickells, T. D., Baker, A. R., Artaxo, P., Benitez-Nelson, C. R., Bergametti, G., Bond, T. C.,
608 Chen, Y., Cohen, D. D., Herut, B., Kubilay, N., Losno, R., Luo, C., Maenhaut, W., McGee, K. A., Okin, G.
609 S., Siefert, R. L. & Tsukuda, S. (2008) 'Global distribution of atmospheric phosphorus sources,
610 concentrations and deposition rates, and anthropogenic impacts'. *Global Biogeochemical Cycles*, 22
611 (4), pp. n/a-n/a.

612

613 Maier, G., Glegg, G. A., Tappin, A. D., & Worsfold, P. J. (2012). A high resolution temporal study of
614 phytoplankton bloom dynamics in the eutrophic Taw Estuary (SW England). *Science of The Total*
615 *Environment*, 434, 228-239.

616

617 Martino, M., Hamilton, D., Baker, A. R., Jickells, T. D., Bromley, T., Nojiri, Y., Quack, B. & Boyd, P. W.
618 (2014) 'Western Pacific atmospheric nutrient deposition fluxes, their impact on surface ocean
619 productivity'. *Global Biogeochemical Cycles*, 28 (7), pp. 712-728.

620

621 Moore, C. M., Mills, M. M., Arrigo, K. R., Berman-Frank, I., Bopp, L., Boyd, P. W., Galbraith, E. D., Geider,
622 R. J., Guieu, C., Jaccard, S. L., Jickells, T. D., La Roche, J., Lenton, T. M., Mahowald, N. M., Maranon, E.,
623 Marinov, I., Moore, J. K., Nakatsuka, T., Oschlies, A., Saito, M. A., Thingstad, T. F., Tsuda, A. & Ulloa, O.
624 (2013) 'Processes and patterns of oceanic nutrient limitation'. *Nature Geosci*, 6 (9), pp. 701-710.

625

626 Myriokefalitakis, S., Nenes, A., Baker, A. R., Mihalopoulos, N. & Kanakidou, M. (2016) 'Bioavailable
627 atmospheric phosphorous supply to the global ocean: a 3-D global modeling study'. *Biogeosciences*,
628 13 (24), pp. 6519-6543.

629

630 Okin, G. S., Baker, A. R., Tegen, I., Mahowald, N. M., Dentener, F. J., Duce, R. A., Galloway, J. N., Hunter,
631 K., Kanakidou, M., Kubilay, N., Prospero, J. M., Sarin, M., Surapipith, V., Uematsu, M. & Zhu, T. (2011)
632 'Impacts of atmospheric nutrient deposition on marine productivity: Roles of nitrogen, phosphorus,
633 and iron'. *Global Biogeochemical Cycles*, 25 (2), pp. n/a-n/a.

634

635 Ottley, C. J. & Harrison, R. M. (1992) 'The spatial distribution and particle size of some inorganic
636 nitrogen, sulphur and chlorine species over the North Sea'. *Atmospheric Environment. Part A. General*
637 *Topics*, 26 (9), pp. 1689-1699.

638

639 Owens, N. J. P., Galloway, J. N. and Duce (1992) 'Episodic atmospheric nitrogen deposition to
640 oligotrophic oceans', *Nature*, 357(6377), pp. 397-399.

641

642 Park, G.-H., Lee, S.-E., Kim, Y.-i., Kim, D., Lee, K., Kang, J., Kim, Y.-H., Kim, H., Park, S. and Kim, T.-W.
643 (2019) 'Atmospheric deposition of anthropogenic inorganic nitrogen in airborne particles and
644 precipitation in the East Sea in the northwestern Pacific Ocean', *Science of The Total Environment*, 681,
645 pp. 400-412.

646

647 Redfield, A. C. (1958) 'THE BIOLOGICAL CONTROL OF CHEMICAL FACTORS IN THE ENVIRONMENT'.
648 *American Scientist*, 46 (3), pp. 230A-221.

649

650 Rees, A. P., Hope, S. B., Widdicombe, C. E., Dixon, J. L., Woodward, E. M. S. and Fitzsimons, M. F. (2009)
651 'Alkaline phosphatase activity in the western English Channel: Elevations induced by high summertime
652 rainfall', *Estuarine, Coastal and Shelf Science*, 81(4), pp. 569-574.

653

654 Schmidt, K., Birchill, A. J., Atkinson, A., Brewin, R. J. W., Clark, J. R., Hickman, A. E., Johns, D. G., Lohan,
655 M. C., Milne, A., Pardo, S., Polimene, L., Smyth, T. J., Tarran, G. A., Widdicombe, C. E., Woodward, E.
656 M. S., & Ussher, S. J. (2020). Increasing picocyanobacteria success in shelf waters contributes to long-
657 term food web degradation. *Global Change Biology*, 26(10), 5574-5587.

658

659 Sharples, J., Moore, C. M., Hickman, A. E., Holligan, P. M., Tweddle, J. F., Palmer, M. R. and Simpson,
660 J. H. (2009) 'Internal tidal mixing as a control on continental margin ecosystems', *Geophysical Research*
661 *Letters*, 36(23).

662

663 Singh, A., Gandhi, N. and Ramesh, R. (2012) 'Contribution of atmospheric nitrogen deposition to new
664 production in the nitrogen limited photic zone of the northern Indian Ocean', *Journal of Geophysical*
665 *Research: Oceans*, 117(C6).

666

667 Slinn, S. A. & Slinn, W. G. N. (1980) 'Predictions for particle deposition on natural waters'. *Atmospheric*
668 *Environment (1967)*, 14 (9), pp. 1013-1016.

669

670 Spokes, L. J. & Jickells, T. D. (2005) 'Is the atmosphere really an important source of reactive nitrogen
671 to coastal waters?'. *Continental Shelf Research*, 25 (16), pp. 2022-2035.

672

673 Spokes, L. J., Yeatman, S. G., Cornell, S. E. & Jickells, T. D. (2000) 'Nitrogen deposition to the eastern
674 Atlantic Ocean. The importance of south-easterly flow'. *Tellus B*, 52 (1), pp. 37-49.

675

676 Statham, P. J. (2012) 'Nutrients in estuaries — An overview and the potential impacts of climate
677 change'. *Science of The Total Environment*, 434 pp. 213-227.

678

679 Wang, Q., Song, J., Li, X., Yuan, H., Li, N., Duan, L. and Ren, C. (2019) 'Geochemical characteristics and
680 potential biogeochemical effect of water-soluble ions in atmospheric aerosols over the western
681 boundary regions of Pacific Ocean', *Atmospheric Research*, 227, pp. 101-111.

682

683 Woodward, E. M. S., Harris, C. (2019) 'Nutrient concentration profiles from long term time series at
684 Station L4 in the Western English Channel from 2000 to 2017'. *British Oceanographic Data Centre*,
685 *National Oceanography Centre, NERC, UK*. doi:10/c2rb.

686

687 Woodward, E. M. S. and Rees, A. P. (2001) 'Nutrient distributions in an anticyclonic eddy in the
688 northeast Atlantic Ocean, with reference to nanomolar ammonium concentrations', *Deep Sea*
689 *Research Part II: Topical Studies in Oceanography*, 48(4), pp. 775-793.

690

691 Yang, M., Bell, T. G., Brown, I. J., Fishwick, J. R., Kitidis, V., Nightingale, P. D., Rees, A. P. and Smyth, T.
692 J. (2019) 'Insights from year-long measurements of air–water CH₄ and CO₂ exchange in a coastal
693 environment', *Biogeosciences*, 16(5), pp. 961-978.

694

695 Yang, M., Bell, T. G., Hopkins, F. E., Kitidis, V., Cazenave, P. W., Nightingale, P. D., Yelland, M. J., Pascal,
696 R. W., Prytherch, J., Brooks, I. M. & Smyth, T. J. (2016a) 'Air–sea fluxes of CO₂ and CH₄ from the Penlee
697 Point Atmospheric Observatory on the south-west coast of the UK'. *Atmos. Chem. Phys.*, 16 (9), pp.
698 5745-5761.

699

700 Yang, M., Bell, T. G., Hopkins, F. E. & Smyth, T. J. (2016b) 'Attribution of atmospheric sulfur dioxide
701 over the English Channel to dimethyl sulfide and changing ship emissions'. *Atmos. Chem. Phys.*, 16 (8),
702 pp. 4771-4783.

703

704 Yeatman, S. G., Spokes, L. J., Dennis, P. F. & Jickells, T. D. (2001) 'Can the study of nitrogen isotopic
705 composition in size-segregated aerosol nitrate and ammonium be used to investigate atmospheric
706 processing mechanisms?'. *Atmospheric Environment*, 35 (7), pp. 1337-1345.

707

708 Yeatman, S. G., Spokes, L. J. & Jickells, T. D. (2001) 'Comparisons of coarse-mode aerosol nitrate and
709 ammonium at two polluted coastal sites'. *Atmospheric Environment*, 35 (7), pp. 1321-1335.

710

711